^{56}Fe capture cross section experiments at the RPI LINAC Center

Brian McDermott[1], Ezekiel Blain[1], Nicholas Thompson[1], Adam Weltz[1], Amanda Youmans[1], Yaron Danon[1], Devin Barry[2], Robert Block[2], Adam Daskalakis[2], Brian Epping[2], Gregory Leinweber[2], and Michael Rapp[2]

[1] Rensselaer Polytechnic Institute, Gaerttner LINAC Center, 110 8th Street, Troy, NY 12180, USA
[2] Bechtel Marine Propulsion Corp., Knolls Atomic Power Laboratory, PO Box 1072 Schenectady, NY 12301-1072, USA

Abstract. A new array of C_6D_6 detectors installed at the RPI LINAC Center has enabled the capability to measure neutron capture cross sections above the 847 keV inelastic scattering threshold of ^{56}Fe through the use of digital post-processing filters and pulse-integral discriminators, without sacrificing the statistical quality of data at lower incident neutron energies where such filtering is unnecessary. The C_6D_6 detectors were used to perform time-of-flight capture cross section measurements on a sample 99.87% enriched iron-56. The total-energy method, combined with the pulse height weighting technique, were then applied to the raw data to determine the energy-dependent capture yield. Above the inelastic threshold, the data were analyzed with a pulse-integral filter to reveal the capture signal, extending the the full data set to 2 MeV.

1. Overview

1.1. Introduction

Modern computational tools have enabled scientists and engineers to perform faster, higher-fidelity simulations of nuclear systems than ever before. The validity of these simulations is ultimately constrained by the quality of the nuclear data they incorporate. Consequently, there is a perennial need for new and improved cross section measurements on a wide variety of isotopes, particularly with regards to capture cross sections in the low keV to the low MeV range.

Iron's role as a structural material in a wide variety of nuclear systems, and as a "seed" nucleus in stellar nucleosynthesis [1], makes it a particularly strong candidate for new and better cross section measurements. However, the upper energy limit for existing capture cross section evaluations in the resolved resonance region of its major isotope, iron-56, has historically been constrained by the first inelastic threshold at 847 keV. Because most differential capture cross-section measurements rely on the detection of prompt γ-ray cascades emitted during the de-excitation of compound nuclei, it is difficult to obtain reliable data above this threshold, as inelastic photons tend to mask the much smaller capture signal.

Through the use of a new C_6D_6 detector array (Fig. 1) developed at the Gaerttner Linear Accelerator Center at Rensselaer Polytechnic Institute (RPI LINAC) [2], new data have been obtained for the capture cross section of ^{56}Fe above the inelastic threshold from 850–2000 keV. The system consists of four C_6D_6 detector modules that have been designed and mounted so as to reduce their sensitivity to scattered neutrons [2]. The data acquisition system is fully-digitized and saves each individual event for off-line processing and analysis. This allows one to apply energy filters and discriminators to regions of the data affected by inelastic scattering without sacrificing the statistical quality of the data where such filtering is not necessary.

1.2. Theory of operation

In any capture measurement, the main criterion for detector performance is insensitivity to the multiplicity and energy spectrum of the capture cascade pathway [3]. This can be achieved with large, 4π detectors that absorb the full energy of the capture cascade [4–6] (*total absorption* detectors), or via detectors that detect a single γ-ray per cascade with a detection efficiency proportional to the γ-ray's incident energy, known as the *total energy* method [7].

The primary assertion made when invoking the total energy method is that the efficiency to detect a single capture cascade photon, η_γ, is proportional to that photon's energy, E_γ (Eq. (1)):

$$\eta_\gamma = kE_\gamma \tag{1}$$

For a detector where only a single γ-ray per cascade is detected (i.e., $\eta_\gamma \ll 1$), the total efficiency to detect a capture event, η_c, can be approximated as a summation of the individual photons' detection efficiencies [7]. Under this assumption, and the assertion in Eq. (1), it can be shown that the efficiency to detect a capture event is proportional to the total excitation energy, E_{ex}, of the compound nucleus, and thus insensitive to the cascade pathway:

$$\eta_c \approx \sum_{i=1}^{m_\gamma} \eta_{\gamma,i} = k \sum_{i=1}^{m_\gamma} E_{\gamma,i} = kE_{ex} \tag{2}$$

The total energy method readily lends itself to the use of low neutron sensitivity detector designs, such as those employing C_6D_6. Since most detectors do not inherently meet the proportionality requirement, post-processing methods are instead applied to the detector

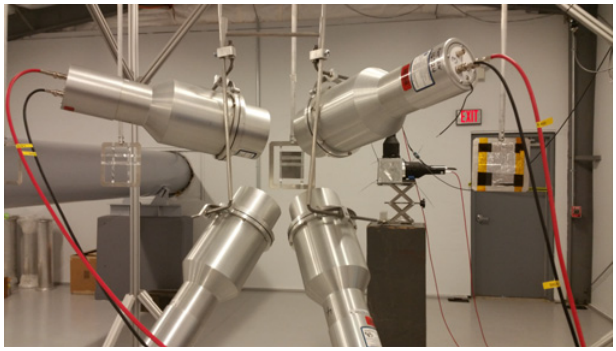

Figure 1. The C_6D_6 experimental setup at the RPI LINAC. The ^{56}Fe sample measured in this work is visible at the center of the detector array.

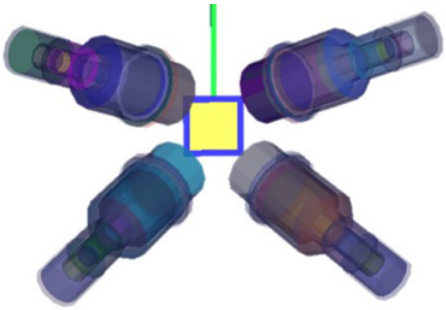

Figure 2. The MCNP geometry of the experimental setup used for weighting function calculations.

response in order to satisfy it. This method, known as the pulse height weighting technique (PHWT), corrects the detectors' response functions $R(E_d, E_\gamma)$ using a weighting function $W(E_d)$, which is determined via experimental measurements and MCNP simulations of the pulse height spectra for a number of different photon energies [7,9,10]. The full expression for the PHWT is given by Eq. (3).

$$kE_\gamma = \eta_\gamma = \int_{E_L}^{\infty} R(E_d, E_\gamma) W(E_d) dE_d. \qquad (3)$$

The weighting function used in this work was taken to be a 5th-order polynomial whose coefficients were calculated using a linear least-squares fit to the MCNP-simulated response functions. Separate weighting functions were found for each detector module, each sample, and each value of the lower level discriminator, E_L, used in the analysis. A detailed model of the experimental setup (Fig. 2) was used in order to accurately simulate photon transport through both the sample and surrounding materials.

2. Experimental methods

The sample chosen for this set of experiments was composed of metallic iron enriched to 99.87% in ^{56}Fe, which had been used and analyzed extensively in prior ^{56}Fe cross section studies at the RPI LINAC [11]. In order to better adapt it to these capture measurements, the original sample was cut into six individual pieces, and assembled into a parallelepiped sample with an areal number density of 0.05159 ± 0.0003 atom/b. Also included in the measurement was a separate 0.181 ± 0.0008 atom/b sample of B_4C, enriched to 91.7% ^{10}B,

Table 1. LINAC Beam Conditions.

Run Date	γ-Flash FWHM [ns]	Observed t_0 [ns]
08/17/2015	8.0 ± 0.4	1868.7 ± 0.8
11/30/2015	8.2 ± 0.3	1868.8 ± 0.8

for the purposes of determining the time-dependent flux shape below 1 MeV via detection of the 478 keV photons emitted in ^{10}B(n, $\alpha\gamma$)^{7}Li reactions. The flux shape above 1 MeV was measured using a 3 mm thick EJ-204 plastic scintillation detector placed 3 m downstream from the sample location. A sample of natural lead with dimensions identical to the iron sample was also measured in order to determine the shape of the time-dependent background resulting from the scattering of in-beam photons into the detector modules. All samples were mounted to the low-mass sample changer at a flight path of 45.28 ± 0.05 m from the neutron-producing LINAC target.

Data were collected in two separate, week-long measurement campaigns using a LINAC pulse frequency of 400 Hz and pulse widths and observed t_0 values listed in Table 1. An 5/32″ (0.397 cm) thick B_4C filter was placed in the beam to remove low energy "overlap" neutrons, as well as 5/8″ of lead to reduce the in-beam photon background.

3. Data reduction & analysis

Following the experiment, several hundred GB of raw digitized detector pulses were processed and reduced to a smaller, 10 GB HDF5 database [12] containing information on time-of-flight (TOF), pulse integral and other parameters needed to perform further analysis. From this database, a querying program was then used to apply filters, invoke the weighting function, and bin the events for each sample into their respective spectra.

The deposited energy of a detector event, E_d, is related to the integral of its ADC sample values, I_{ADC}, via a linear relation.

$$E_d = aI_{ADC} + b. \qquad (4)$$

The parameters a and b in Eq. (4) are determined by measuring the detectors' pulse-integral response to a set of standard γ-emitting calibration sources and performing a least-squares fit. The events are then weighted using the calculated energy value, then binned by TOF.

3.1. Pulse filtering

Multiple analyses of the data were performed in which different values of the lower level discriminator, E_L were applied to the data. Below the 847 keV inelastic threshold, a discriminator of $E_L = 150$ keV was applied to minimize the statistical fluctuations in the data due to counting statistics. Above 847 keV, a value of $E_L = 1$ MeV was used to eliminate the inelastic scattering signal, which consisted entirely of monoenergetic 847 keV photons. The remaining signal after applying this cutoff was that attributable to capture reactions in ^{56}Fe. Because of the high enrichment of the sample, inelastic contributions from other minor isotopes of iron, such as the 1410 keV inelastic state in ^{54}Fe, were assumed to be negligible.

^{56}Fe is unique in that nearly all of its cascades contain a single strong transition to either the ground state or low-lying states just above the ground state [13]. Thus,

this cutoff method can be applied without significantly biasing the measurement due to the inadvertent removal of high-multiplicity transitions consisting only of low-energy photons.

3.2. Background subtraction

The time-dependent photon background associated with the LINAC beam is attributable primarily to 2.2 MeV γ-rays emitted in ^{1}H(n, γ)^{2}H events occurring in the aqueous target moderator, as well as 1–2 MeV photons emitted in the de-excitation of ^{181}Ta in the target itself [14]. A sample of natural lead was measured during the experiment to determine the time-profile of this background. Because lead has a very low capture cross section, and because the detector system's sensitivity to scattered neutrons was found to be negligible based on prior MCNP simulations and scattering measurements performed with lead and carbon [2], it was assumed that the detected signal from the lead sample was attributable solely to in-beam photons scattering into the detectors.

To account for the different photon interaction properties of iron and lead, a correction factor, k_p, was introduced as a normalization factor for the lead data-derived spectrum shape. This normalization factor was found by performing MCNP simulations of $E_\gamma = 2$ MeV photons incident on the lead and iron samples, and taking F8 tallies to construct the subsequent detector response functions, $R(E_d, E_\gamma)$. These responses were then weighted using the weighting functions calculated previously, $W(E_d)$, then integrated from a lower energy limit of E_L and corrected for the ratio of the samples' respective areas, A. The full expression for k_p is given by:

$$k_p(E_\gamma) = \frac{A_{Pb}}{A_{Fe}} \frac{\int_{E_L}^{\infty} W_{Fe}(E_d) R_{Fe}(E_d, E_\gamma) dE_d}{\int_{E_L}^{\infty} W_{Pb}(E_d) R_{Pb}(E_d, E_\gamma) dE_d}. \quad (5)$$

After determining k_p for 2 MeV photons, the full expression for the time-dependent background rate is expressed as:

$$\dot{B}_i = k_p(\dot{C}_{Pb,i} - \dot{B}_0), \quad (6)$$

where $\dot{C}_{Pb,i}$ represents the weighted, flux monitor normalized count rate in the lead in the ith TOF spectrum bin, and $\dot{B}_0$ represents the time-independent, ambient background.

3.3. Flux

The neutron flux shape at energies below 1 MeV, ϕ^{lo}, was determined by measuring the characteristic 478 keV γ-ray from the ^{10}B(n, $\alpha\gamma$)^{7}Li reaction in the B_4C sample described in Sect. 2. The relative time-dependent flux shape is given by:

$$\phi_i^{lo} = \frac{\dot{C}_{B_4C,i} - \dot{B}_i}{Y_{B_4C,i}}, \quad (7)$$

where $\dot{C}_{B_4C,i}$ represents the monitor normalized counting rate in the B_4C sample, $\dot{B}_i$ represents the background counting rate as determined by measurements on an open sample frame, and $Y_{B_4C,i}$ represents the reaction yield of the ^{10}B(n, $\alpha\gamma$)^{7}Li reaction, all of which are evaluated at the ith spectrum bin. Y_{B_4C} is calculated *a priori* via MCNP simulation to fully account for multiple scattering in the sample.

At energies above 1 MeV, competing photon-production reactions in the B_4C sample make it impractical for flux measurement purposes. Instead, a 3 mm EJ-204 proton recoil detector, placed in the beam 3 m downstream from the sample, was used to measure the flux shape in this region, ϕ^{hi}, which, in this arrangement, is given by:

$$\phi_i^{hi} = \frac{\dot{C}_{\text{EJ-204},i}}{\eta_{\text{EJ-204},i}} \quad (8)$$

where $\dot{C}_{\text{EJ-204},i}$ is the count rate in the EJ-204 detector, and $\eta_{\text{EJ-204},i}$ is the relative efficiency of the detector, both evaluated at the ith spectrum bin. The neutron energy dependent behavior of $\eta_{\text{EJ-204},i}$ was characterized via measurements of the ^{252}Cf prompt fission neutron spectrum using a small TOF setup [15]. Background contributions in the EJ-204 were neglected, and instead considered as a source of systematic uncertainty, as they contributed only 1–5% of the total counts in the energy region of interest.

3.4. Capture yield

After determining the background and flux shapes, the full experimental yield for the ith TOF bin is then given by:

$$Y_{i,exp} = f_n \frac{\dot{C}_{Fe,i} - \dot{B}_i - \dot{B}_0}{\phi_i}, \quad (9)$$

where $\dot{C}_{Fe,i}$ represents the count rate in the ^{56}Fe sample, f_n is a normalization constant and all other terms are the same as defined in earlier sections. The data in this measurement are normalized at the 1.15 keV ($\ell = 1$) resonance in ^{56}Fe. To verify that the higher discriminator thresholds did not bias the data by removing important γ-ray transitions, the normalized capture yield spectra for each discriminator setting were compared in the range of 100 to 800 keV, and were found to be in agreement to within the observed statistical uncertainty [16].

4. Results

Capture yields were measured in the ^{56}Fe sample from 1 keV to 2 MeV, and new capture data were observed above 847 keV by applying the methods described in Sect. 3.1. At these high energies, the capture cross section, σ_γ is on the order of 3 mb, while the scattering cross section is on the order of 1–2 b. The contribution to the measured capture yield from neutrons that have undergone one or more scatterings prior to capture was calculated to be on the order of 22% using MCNP. The capture yield was then converted to cross section via Eq. (10), where N is the number density of the sample in atom/b and k_s is the multiple scattering correction factor, which is simply given by the ratio of the analytically-calculated primary capture yield to the MCNP-calculated capture yield using the ENDF/B-VII.1 evaluation.

$$\sigma_\gamma = \frac{Y_\gamma}{k_s N}, \quad (10)$$

Figure 3 shows the preliminary results of this experiment compared with the results of Diven, Stavisskii, and Malyshev [17, 18], which were the only experimental capture data for ^{56}Fe above the inelastic threshold available

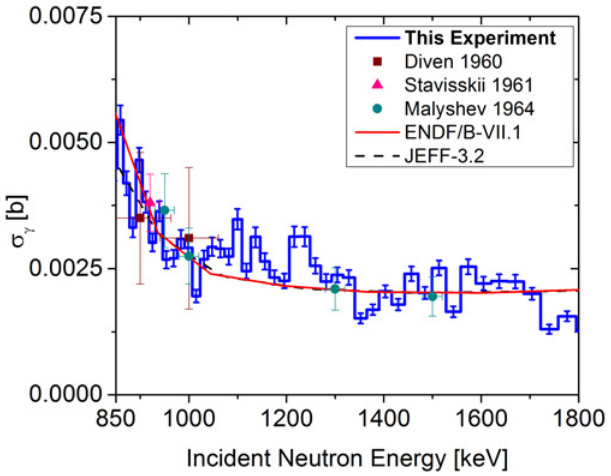

Figure 3. ^{56}Fe capture cross section from 850–2000 keV. The error bars indicate the 1σ uncertainty level. Partially resolved resonance structure is observed in this region.

at the time of this measurement. After applying the multiple scattering correction, the datasets are in very good agreement. The ENDF/B-VII.1 and JEFF-3.2 evaluations are also plotted in Fig. 3, and agree well with the data below 1725 keV.

5. Conclusion

The new C_6D_6 system at the RPI LINAC has provided new experimental capture data for ^{56}Fe above the inelastic threshold, which had previously been sparse. The data agree well with previous measurements, as well as with the evaluations below 1725 keV. At higher energies, the measured data are lower than the present ENDF-B/VII.1 and JEFF-3.2 evaluations, and the lower values are being examined further in support of the final analysis in Ref. [16].

References

[1] E.M. Burbridge, G. Burbridge, W. Fowler, F. Hoyle, Rev. Mod. Phys. **29**, 548 (1957)
[2] B. McDermott, E. Blain, A. Daskalakis, N. Thompson, A. Youmans, H. Choun, W. Steinberger, Y. Danon, M. Rapp, G. Leinweber et al., *Capture Cross Section Measurements in nat-Fe and ^{181}Ta from 1 to 2000 keV using a new C_6D_6 Detector Array*, in *Proceedings of the 2015 International Conference on Criticality Safety* (Charlotte, NC, 2015)
[3] F. Corvi, *The Measurement of Neutron Capture Cross Sections via Prompt Gamma-Ray Detection*, in *Proceedings Specialists Meeting on Measurement, Calculation and Evaluation of Photon Production Data* (Report NEA/NSC/DOC, Bologna, 1994), **95**, 229–246
[4] N. Drindak, Masters, Rensselaer Polytechnic Institute, Troy, NY (1987)
[5] C. Guerrero, U. Abbondanno, G. Aerts, H. Alvarez, F. Alvarez-Velarde, Nucl. Instrum. Meth. A **608**, 424 (2009)
[6] R. Reifarth, T. Bredeweg, A. Alpizar-Vicente, J. Browne, Nucl. Instrum. Meth. A **531**, 530 (2004)
[7] A. Borella, G. Aerts, F. Gunsing, M. Moxon, P. Schillebeeckx, R. Wynants, Nucl. Instrum. Meth. A **577**, 626 (2007)
[8] M. Moxon, E. Rae, Nucl. Instrum. Meth. **24**, 445 (1963)
[9] G. Aerts, E. Berthoumieux, F. Gunsing, L. Perrot, *Weighting functions for the neutron capture measurements performed at nTOF-CERN in 2002–2003* (2004)
[10] The X-5 Monte Carlo Team, *Monte Carlo Team, MCNP – a general purpose Monte Carlo N-particle transport code, version 5* (2003)
[11] H. Liou, R. Chrien, R. Block, U. Singh, Nucl. Sci. Eng. **70**, 150 (1979)
[12] The HDF Group, *Hierarchical Data Format, version 5* (1997), `http://www.hdfgroup.org/HDF5/`
[13] R. Firestone, K. Abusaleem, M. Basunia, F. Bečvář, T. Belgya, Nucl. Data. Sheets **119**, 79 (2014)
[14] J. Tuli, Nucl. Instrum. Meth. A **369**, 506 (1996)
[15] E. Blain, Doctoral Thesis, Rensselaer Polytechnic Institute, Troy, NY (2014)
[16] B. McDermott, Doctoral Thesis, Rensselaer Polytechnic Institute, Troy, NY (2016)
[17] B. Diven, J. Terrell, A. Hemmendinger, Phys. Rev. **120**, 556 (1960)
[18] A.V. Malyshev, Y. Stavisskii, A.V. Shapar, Sov. Atom Energy **17**, 1277 (1964)